Allelopathic studies with furanocoumarins isolated from *Ducrosia anethifolia*. *In vitro* and *in silico* investigations to protect legumes, rice and grain crops

Francisco J. Rodríguez-Mejías [a,b,*], Javad Mottaghipisheh [b,c,d], Stefan Schwaiger [b], Tivadar Kiss [c], Dezső Csupor [c,e], Rosa M. Varela [a,**], Francisco A. Macías [a]

[a] *Allelopathy Group, Department of Organic Chemistry, Institute of Biomolecules (INBIO), Campus CEIA3, School of Science, University of Cádiz, C/ República Saharaui, 7, 11510, Puerto Real (Cádiz), Spain*

[b] *Institute of Pharmacy/Pharmacognosy, Center for Molecular Biosciences Innsbruck (CMBI), University of Innsbruck, CCB, Innrain 80/82, 6020, Innsbruck, Austria*

[c] *Institute of Pharmacognosy, University of Szeged, Eötvös u. 6, H-6720, Szeged, Hungary*

[d] *Department of Aquatic Sciences and Assessment, Swedish University of Agricultural Sciences, SE, 75007, Uppsala, Sweden*

[e] *Institute of Clinical Pharmacy, University of Szeged, Szikra u. 8, H-6725, Szeged, Hungary*

ARTICLE INFO

ABSTRACT

Six different furanocoumarins were isolated from the aerial parts of *Ducrosia anethifolia* and tested *in vitro* for plant cell elongation in etiolated wheat coleoptile. They were also tested for their ability to control three different weeds: ribwort plantain, annual ryegrass, and common purslane. These compounds exhibited strong inhibition of plant cell elongation. In the case of (+)-heraclenin, the IC$_{50}$ was lower than 20 µM, indicating a better inhibition than the positive control Logran®. Computational experiments for docking and molecular dynamics revealed for the investigated furanocoumarins bearing an epoxide moiety an improved fitting and stronger interaction with the auxin-like TIR1 ubiquitin ligase. Furthermore, the formed inhibition complex remained also stable during dynamic evaluation. Bidental interaction at the active site, along with an extended hydrogen-bond lifetime, explained the enhanced activity of the epoxides. The *in vitro* weed bioassay results showed that *Plantago lanceolata* was the most affected weed for germination, root, and shoot development. In addition, (+)-heraclenin displayed better inhibition values than positive control even at 300 µM concentration.

1. Introduction

The search for new sustainable approaches in plant protection led also to the investigations of natural products that can be employed as new lead structures for further development of bioherbicides.

Green approaches in agriculture have been encouraged by institutions and governments all over the world, as an answer for problems observed by the employment of classical herbicides (European Commission, 2021). Most of these classic herbicides are based on highly persistent chemicals, accumulating in soil and water. Additionally, their activity is based on a limited number of possible target interactions, resulting in resistance phenomena. However, it is really important to keep and enhance the yield of relevant crops for human consumption.

Considering rice, grain, and legumes as some of the most important, ribwort plantain (*Plantago lanceolata*), annual ryegrass (*Lolium rigidum*), and common purslane (*Portulaca oleracea*) are some of the most invasive for them, respectively. Natural products, directly linked with allelopathy, have emerged as new strategy to avoid these problems and supersede the current herbicides (Macías et al., 2007).

Among different compound classes of natural product with application in agrochemistry, furanocoumarins have been selected by experts in the field as one of the future bioherbicide leads (Macías et al., 2019). Previous studies have shown interesting results of these coumarins as phytotoxic components. For example, Nebo et al. have shown that chalepsin is highly effective in inhibiting the root formation of standard target species as *Lepidium sativum* (Nebo et al., 2014). In addition,

Meepegala et al. reported the growth inhibition of the dicot *Lactuca sativa* (lettuce) by 8-(3-methylbut-2-enyloxy)-marmesin acetate (Meepegala et al., 2021). Sondhia et al. were more focused on applications against *Agrostis stolonifera* and *Lemna paucicostata* weeds, and showed the efficacy of imperatorin, (+)-heraclenin, and (+)-heraclenol against them (Sondhia et al., 2012).

Ducrosia anethifolia is an interesting species from the Apiaceae family, which has provided new phytochemicals in recent years. This is the case of the monoterpene ducrosin A and sesquiterpene ducrosin B which can be isolated from the dichloromethane extract of fruit (Oueslati et al., 2019). This plant is native to Afghanistan, Gulf States, Iran, Iraq, Lebanon-Syria, Oman, Pakistan, Palestine, Saudi Arabia, Yemen, mainly observed in the subtropical/steppe areas and cohabit with most of the Mediterranean crops of interest. In terms of furanocoumarins, Mottaghipisheh et al. (2018), as well as Shalaby et al. (2014), have obtained psoralen, 5-methoxypsoralen, 8-methoxypsoralen, imperatorin, and isooxypeucedanin among other furanocoumarins from the aerial parts of this plant.

From the allelopathic point of view, the biological targets of coumarins and derivatives in plant cells have been also explored. Dihydrocoumarins have been found to act in hormones transduction and as phenylpropanoid biosynthesis genes inhibitors in *Echinochloa crus-galli*, specifically for PAL and 4CL genes (Yang et al., 2022). In case of furanocoumarins, auxin-like receptors were identified as the main target for scopoletin according to the studies of Graña et al. (2017). Auxin has long been recognized as an important phytohormone that regulates plant growth in response to diverse developmental and environmental cues. The major naturally occurring auxin, indole-3-acetic acid (IAA), coordinates many plant growth processes by modulating gene expression, which leads to changes in cell division, elongation and differentiation. Their investigations revealed strong cell and tissue abnormalities on treated roots, such as cell wall malformations, multi-nucleated cells, abnormal nuclei, and tissue disorganization of *Arabidopsis thaliana* cells. 2,4-D was employed a positive control due to structural similarities to scopoletin and both displayed to fit into the auxin-binding site TIR1 (Graña et al., 2017). This site is placed at the center of the signaling cascade of the auxin signaling pathway and it has a key role in sensing and transducing the hormone signal to transcriptional programs. Recently, it has been demonstrated that auxin binds directly to SCF^{TIR1} and promotes the interaction between TIR1 and auxins (Fendrych et al., 2018).

In this work, we have isolated six different furanocoumarins from aerial parts of *Ducrosia anethifolia*: bergapten, imperatorin, (+)-oxypeucedanin, (+)-heraclenol, (+)-heraclenin, and (+)-isogospherol, and different phytotoxic *in vitro* studies were performed. Firstly, a general phytotoxic analysis in etiolated wheat coleoptile, and after that a specific bioassay against ribwort plantain (*Plantago lanceolata*), annual ryegrass (*Lolium rigidum*), and common purslane (*Portulaca oleracea*). Germination, root formation, and shoot growth were analyzed in these three highly problematic weeds, as a result of their abundance around several key crops, namely wheat, tomatoes, and beans (Mejías et al., 2022a,b,c). Finally, *in silico* docking studies and molecular dynamics have been performed to evaluate the mode of action by inhibition of the auxin-binding site TIR1.

2. Results and discussion

The employed phytochemical protocol utilizing the methanolic extract of the aerial parts of *Ducrosia anethifolia* resulted in a limited amount of pure compounds: 14.0 mg of bergapten (**1**), 1.4 mg of imperatorin (**2**), 14.3 mg of (+)-oxypeucedanin (**3**), 2.6 mg of (+)-heraclenol (**4**), 1.6 mg of (+)-heraclenin (**5**), and 2.3 mg of (+)-isogospherol (**6**). Furanocoumarins are the major phytoconstituents of *D. anethifolia* and *D. ismaelis*. They were most abundant in chloroform extracts of the aerial parts, including stem, leaf and seed, but also easily found in methanolic extracts. All compounds obtained were characterized and identified according to reported data (Fig. 1) (Banerjee et al., 1987; Setzer et al., 2003; Stevenson et al., 2003; Sultana and Sultana, 2009; Wei and Ito, 2006).

The coleoptile bioassay was carried out to evaluate the general phytotoxicity of the isolated furanocoumarins. The compounds were added to the coleoptile segment of the wheat, with 24 h of exposure time. It can be observed that **1** is not active in comparison to other furanocoumarins. Bergapten (**1**) bears the shortest ether functionalization chain (-OCH$_3$) among the tested compounds and therefore a lack of freedom degrees for the side chain, that could influence the bioactivity. Attending to Tice's rule for herbicides displayed in Table 1, a direct relationship among activity, rotatable bonds, number of hydrogen bond acceptors and donors and mLog$P$ can be observed (Yadav et al., 2015). None of them violate the rule, but in case of (+)-oxypeucedanin (**3**), (+)-heraclenin (**5**) and (+)-isogospherol (**6**) their values are close to the optimum, which is half of the maximum, as shown by IC$_{50}$ values lower than 30 μM. Specifically, Fig. 3 shows a parabolic relationship between the IC$_{50}$ and rotatable bonds with a goodness of fit of 0.996 for the six tested furanocoumarins according to Hansch's nonlinear model (Durán et al., 2018; Hansch and Fujita, 1964). Fig. S1 displays the representation of the data together with the theoretical representation according to Hansch's nonlinear model for better understanding of the fit. Therefore, freedom degrees in the side chains will allow better interactions with the molecular target.

(+)-Heraclenin (**5**) shows the best IC$_{50}$ value, but activity displayed for 1000, 300, and 100 μM are not the highest. However, activity at 30 μM surpass 50% of inhibition in wheat coleoptiles. This is the typical profile for poor soluble compounds and it would be interesting to perform a future bioassay improving its physicochemical properties. In addition, for lower concentrations (30 μM and 10 μM), inhibition displayed for all the furanocoumarins are stronger than both positive controls.

A significant difference in coleoptile inhibition is observed between imperatorin (**2**) and (+)-isogospherol (**6**), despite the fact that their structural arrangement differs only in the presence of a hydroxyl group and double bond isomerism. This difference is more than 10 units of activity for all the concentration tested, and more than 20 units specifically for 300 μM. According to Fig. 1, the mLog$P$ values show differences greater than one unit, indicating that the solubility of the molecules influences their activity. However, what is most interesting between the two compounds is that the number of rotatable bonds increases with isomerism in the double bond. The isogospherol (**6**) now has a new rotatable bond as the double bond becomes terminal, and this influences the activity.

Another interesting fact is the influence of the position of the epoxide in furanocoumarin. (+)-Oxypeucedanin (**3**) and (+)-heraclenin (**5**) differ in the maximum inhibition achieved at the two highest concentrations by more than a 15% difference. These differences at 1000 μM and 300 μM are significant with 99% and 98% of confidence according to Welch's *t*-test. The differences between the substitution at 5 (opposite the lactone ring) and position 8 (same side as the lactone ring) are clarified here. Position 5 generates a stronger interaction at higher concentrations, but leads to a rapid loss of inhibition for low concentrations. This is not the case for position 8 (**5**), since its activity remains high even at low concentrations, as seen in the IC$_{50}$ values in Fig. 3. This type of behavior presented by **3**, with substitution at position 5, usually corresponds to reversible inhibitors or non-covalent interactions at the site of action, in contrast to that observed with substitution at position 8.

Figure S2 show slight macroscopic differences for wheat coleoptiles treated with different furanocoumarins and the positive control. Figure S2-A shows the length of the coleoptile when 1000 μM concentration of bergapten (**1**) is tested, and Figure S2-B displays the length at the same concentration when (+)-oxypeucedanin (**4**) is evaluated. The appearance of the coleoptile in both images are rather the same, and only the length is different, pointing to a stronger inhibition of the proteins involved in the development. However, the appearance of
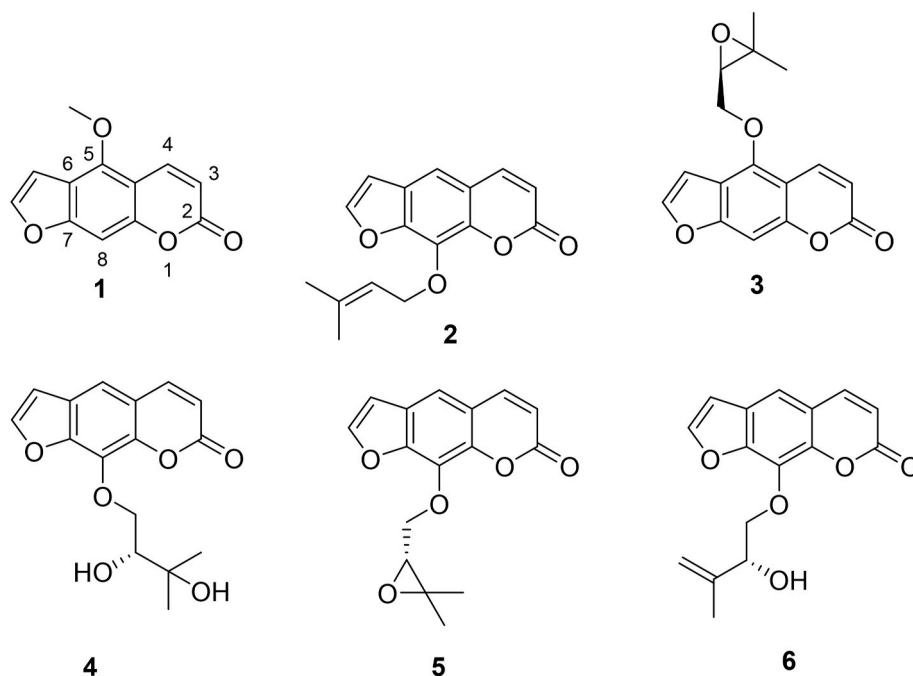
Fig. 1. Structures of furanocoumarins isolated and biologically tested.

coleoptiles treated with StompAqua® is quite different. Figure S2-C shows a yellowing process, which is usually associated with urea-based herbicides like pendimethalin, directly linked with interferences with the fatty acid synthesis for plant cell membranes (Monaco et al., 2002). Those differences indicate therefore a difference in the respective mode of action. Specifically, furanocoumarins are described as TIR1 inhibitors, which is part of the Skp1-Cul1-F-box (SCF) ubiquitin ligase family and plays a role in the auxin signaling. This allows for the regulation of diverse auxin-mediated processes including root growth and development, shoot development, and apical dominance (Cardozo and Pagano, 2004; Dharmasiri et al., 2005).

To evaluate the SAR of furanocoumarins for the inhibition of TIR1, *in silico* molecular docking experiments were performed. Although currently no co-crystal structures with the physiological ligands nor an inhibitor are available, the putative binding side was localized by comparison of different mutants and their sensitivity towards 2,4-D or IAA (Walsh et al., 2006). Since scopoletin was suggested to bind analogously to 2,4-D, scopoletin conformation, interaction and score values were employed as positive control. According to Figure S3, it can be observed that most of the *in silico* experiments are in agreement with the bioactivity profile displayed in the *in vitro* etiolated wheat coleoptile assay, which is used to monitor the inhibition of TIR1 ubiquitin ligase. Bergapten (1) revealed the lowest score value in comparison to other furanocoumarins, and the same behavior is displayed in the wheat coleoptile bioassay. However, the score displayed for (+)-heraclenol (4) is smaller than expected. As shown in Fig. 1, (+)-heraclenol bears two hydroxyl groups instead of a closed epoxide system, as observed in (+)-oxypeucedanin (3) and (+)-heraclenin (5). The main difference associated with this compound is the possible presence of an intramolecular of hydrogen bond between hydroxyl group at C3″ and the ether oxygen of the lactone moiety, as observed in Figure S4. This would prevent intermolecular interactions with amino acid residues of TIR1, decreasing the *in silico* activity.

Analysis of theoretical furanocoumarin interactions shows that substitution in position 5 (opposite side as the lactone group) generates less interactions than position 8 substitutions (same side as lactone moiety and furan ring oxygen). For example, in case of (+)-heraclenin (5), (Fig. 4-A), a bidentate interaction among arginine489, epoxide group, and ester scaffold is observed. In case of bergapten (1), (Fig. 4-C),

the lack of π-interaction with amino acid residues, which generates a lower score in the docking simulations, can be observed. This compound also presents a smaller number of rotatable bonds, which in agreement with Fig. 3, and should display the lowest value of interactions.

To evaluate the stability of the inhibition complex generated, molecular dynamics *in silico* studies were performed. Since the most interesting results were expected for the comparison of compounds with a high and low activity bergapten (1) was selected as representative of the less active compounds in the wheat coleoptile *in vitro* bioassay, bearing a lower number of rotatable bonds in the side chain, and lower score in TIR1 inhibition simulation. On the other hand, (+)-oxypeucedanin (3) was selected as one of the most active compounds, experimentally and theoretically. Fig. 5 shows the difference between bergapten (1) and (+)-oxypeucedanin (3) in terms of stability by RMSD analysis of the ligand and the complex, as well as the energy evolution along the simulation period. RMSD plot displays a quite robust complex generated for both furanocoumarins, with fluctuations below 2.0 Å, which is the commonly accepted maximum tolerance to determine stability of the complex (Mejías et al., 2022a,b,c). However, after 30 ns, the bergapten (1) interaction site undergoes a continuous fluctuation attributed to conformational changes. According to Figure S5, changes at the bergapten location are smaller and main modification is owing to the rotatable methoxy group. In comparison with (+)-oxypeucedanin, bergapten shows a lower stability of the inhibition complex, which has an impact on the interaction energy observed in the right diagram of Fig. 5. During the simulation, bergapten always showed a more positive interaction energy than (+)-oxypeucedanin, explaining the lowest activity of 1 observed in Fig. 2.

Average energy values of the complex according to Lennard-Jones potential are -86.321 ± 2.713 kJ/mol for bergapten (1) and -106.639 ± 2.146 kJ/mol for (+)-oxypeucedanin (3), as expected according to previous experimental results displayed. Major contribution for this energy can be attributed to intermolecular hydrogen bonds with TIR1. Fig. 6 shows the analysis of the different number hydrogen bonds along the 50 ns simulations and reveals for (+)-oxypeucedanin a higher number of bonds, especially in case of the long donor-acceptor distance. Furthermore, average number of this kind of bonds and the lifetime are also higher than in case of bergapten (1). Both facts are directly linked with the stability and energy of the complex and could explain

Table 1
Tice's rules evaluation of isolated furanocoumarins.

No	Furanocoumarin	Molecular Formula	Tice's rule	
			Properties	Value
1	Bergapten	$C_{12}H_8O_4$	M.W. ($\leq$500 amu)	216.19
			mLog$P$ ($\leq$5)	2.28
			H-bond donors ($\leq$3)	0
			H-bond acceptors ($\leq$12)	4
			Rotatable bonds ($\leq$12)	1
			IC$_{50}$ (μM) (wheat coleoptile)	–
2	Imperatorin	$C_{16}H_{14}O_4$	M.W. ($\leq$500 amu)	270.28
			mLog$P$ ($\leq$5)	3.95
			H-bond donors ($\leq$3)	0
			H-bond acceptors ($\leq$12)	4
			Rotatable bonds ($\leq$12)	3
			IC$_{50}$ (μM) (wheat coleoptile)	89.93 $\pm$ 9.63
3	(+)-Oxypeucedanin	$C_{16}H_{14}O_5$	M.W. ($\leq$500 amu)	286.25
			mLog$P$ ($\leq$5)	2.98
			H-bond donors ($\leq$3)	0
			H-bond acceptors ($\leq$12)	5
			Rotatable bonds ($\leq$12)	3
			IC$_{50}$ (μM) (wheat coleoptile)	26.06 $\pm$ 2.15
4	(+)-Heraclenol	$C_{16}H_{16}O_6$	M.W. ($\leq$500 amu)	304.30
			mLog$P$ ($\leq$5)	1.81
			H-bond donors ($\leq$3)	2
			H-bond acceptors ($\leq$12)	6
			Rotatable bonds ($\leq$12)	4
			IC$_{50}$ (μM) (wheat coleoptile)	56.48 $\pm$ 6.02
5	(+)-Heraclenin	$C_{16}H_{14}O_5$	M.W. ($\leq$500 amu)	286.28
			mLog$P$ ($\leq$5)	2.92
			H-bond donors ($\leq$3)	0
			H-bond acceptors ($\leq$12)	5
			Rotatable bonds ($\leq$12)	3
			IC$_{50}$ (μM) (wheat coleoptile)	17.18 $\pm$ 5.51
6	(+)-Isogospherol	$C_{16}H_{14}O_5$	M.W. ($\leq$500 amu)	286.28
			mLog$P$ ($\leq$5)	2.82
			H-bond donors ($\leq$3)	1
			H-bond acceptors ($\leq$12)	5
			Rotatable bonds ($\leq$12)	4
			IC$_{50}$ (μM) (wheat coleoptile)	27.42 $\pm$ 7.13

*IC$_{50}$ (wheat coleoptile) of positive control Logran®: 40.1 μM.

theoretically the results observed experimentally for the inhibition of the wheat coleoptile growth.

Fig. 7 displays the snapshots for the molecular dynamic interaction between (+)-oxypeucedanin (**3**) and TIR1 ubiquitin ligase. In contrast to the RMSD plot (Fig. 5), the stability of the complex shows less fluctuations during most of the time of the molecular dynamic simulation. After 5 ns, a +0.6 Å RMSD in the complex can be observed, which is explainable by the rotation of the side chain according to the shown differences between snapshot at 0 ns and 10 ns in Fig. 7. However, after this period, no more modifications are observable and fluctuations are quite stable until 50 ns. This could be related to bidental interactions of epoxide, ester and amino acid residues previously mentioned at the *in silico* docking experiment section.

In silico tests have highlighted that TIR1 could be a target related to the growth and development of the plants evaluated. However, this auxin receptor belongs to a big family of auxin-regulated mediators like AFB1 and AFB3, which could be also affected by furanocoumarins.

In vitro tests were conducted against ribwort plantain (*Plantago lanceolata*), annual ryegrass (*Lolium rigidum*), and common purslane (*Portulaca oleracea*) using bergapten (**1**), (+)-oxypeucedanin (**3**), (+)-heraclenol (**4**), and (+)-heraclenin (**5**) (Figure S6). Ribwort plantain usually affects to the yield of legume crops and pastures, as alfalfa, beans, chickpeas (Mejías et al., 2022a,b,c; Russell et al., 2021). Common purslane is really problematic for rice crops (Tabaglio et al., 2008). Annual ryegrass infects most of grain crops, mainly barley and wheat (Macías et al., 2006).

Bergapten and (+)-oxypeucedanin were selected for specific bioassays due to their different functionalization at position 5. On the other hand, (+)-heraclenol and (+)-heraclenin were examined to assess the structure-activity relationship, focusing on differences in functionalization at position 5 and 8, as well as the disparity between epoxide and hydroxyl activity.

According to the *in silico* investigations (Figure S3 and Fig. 5), the epoxide derivatives consistently exhibited higher activity than the hydroxyl derivatives, regardless of the position of the substituent. However, *in vitro* coleoptile bioassays showed contrasting results, with (+)-heraclenol displaying stronger inhibition than the epoxide at higher concentrations, despite (+)-heraclenin demonstrating a better IC$_{50}$ value. It is possible that a chemical modification of the epoxide to a hydroxyl derivative occurs upon incorporation into plant tissues. Additionally, the permeability of weed seeds poses a significant barrier to activity, and epoxide and hydroxyl furanocoumarin derivatives may interact differently during the cross-membrane process. As a result, *in vitro* tests may exhibit different behavior than what is observed in *in silico* evaluations, potentially showing high activity for hydroxylated compounds.

In the case of *L. rigidum*, no or only a weak inhibition was observed for germination inhibition with the tested compounds, but with a good response to the positive control StompAqua®. This differs from the impact on the germination inhibition of *P. lanceolata* and *P. oleracea*, which are both dicots, which responded barely to the positive control but strongly to the furanocoumarins in the case of *P. lanceolate* and only weak in the case of *P. oleracea*. Therefore, it appears that these furanocoumarins show a specific clade selectivity. Another factor might be differences in the permeability of the seeds/fruits attributed to climate adaptation. *P. oleracea* is native to dry climates, specifically the top and central parts of Africa, while *P. lanceolata* thrives in wetter climates such as Europe and Northern Asia. (Royal Botanic Garden, 2023a,b) Morphologically, *P. lanceolata* seeds have an elliptical shape with a seed length of 2.39 $\pm$ 0.01 mm and seed breadth of 1.06 $\pm$ 0.11 mm. The length of seed coat cells is 50.67 $\pm$ 1.15 μm, and the breadth of seed coat cells is 29.00 $\pm$ 1.02 μm (Verma and Kumar Avinash Bharti, 2017). On the other hand, *P. oleracea* seeds exhibit a circular-ovate shape with a seed length of 0.91 $\pm$ 0.06 mm and seed breadth of 0.97 $\pm$ 0.06 mm (Kim, 2012). So, the interaction surface of the *P. lanceolata* seeds with the compound solutions would be higher, enhancing the action. However, there is limited available data on coat cells in the literature. According to Danin et al., the conditions for germination of *P. oleracea* differ, as the germination water needs to penetrate not only the seed coat but also the calyptra (Danin et al., 1978).

As it was previously mentioned, *Lolium rigidum* belongs to monocots clade. Most of the herbicide from industry are focus on one clade due to big systematic and molecular differences (Broster et al., 2013). Specifically, they respond differently to auxinic herbicides (McSteen, 2010). This seem to be the case of tested furanocoumarins according to *in silico* results and what is observed in Fig. 8. In addition to this, germination of *L. rigidum* can also be affected because of morphological aspect, as well as characteristic dormancy observed in this kind of cereal caryopses (Goggin and Powles, 2012) *L.. rigidum* has fusiform caryopses between 2.7 and 5.5 mm, at least three times longer than wide. (Maity et al.,
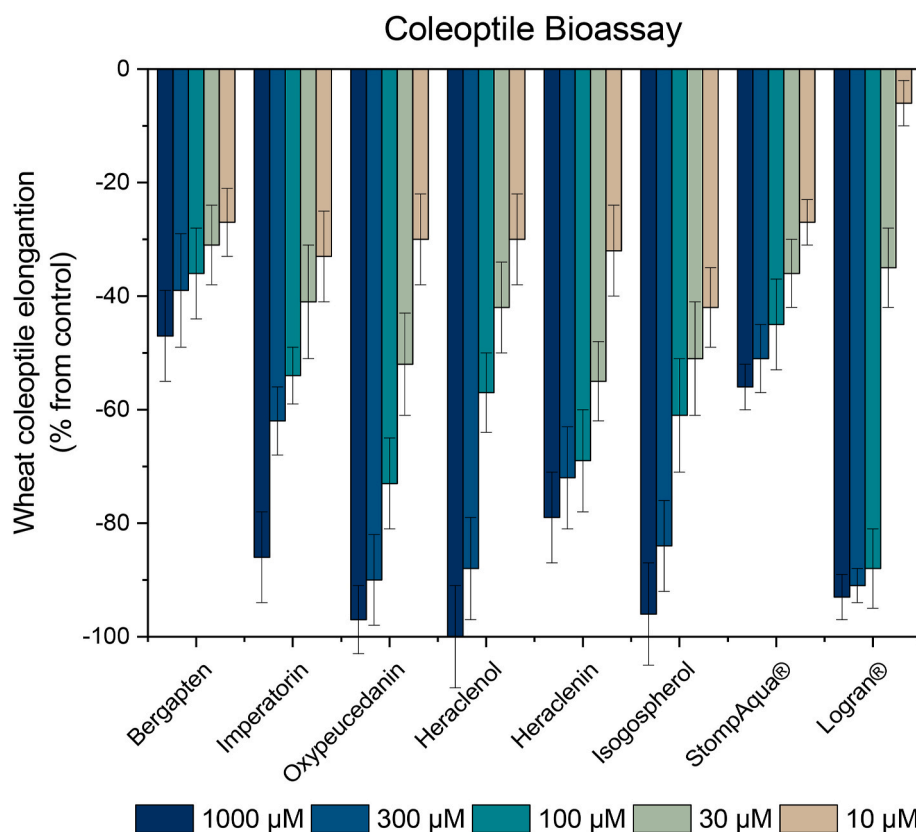
Fig. 2. Bioassay result for etiolated wheat coleoptiles of bergapten (**1**), imperatorin (**2**), (+)-oxypeucedanin (**3**), (+)-heraclenol (**4**), (+)-heraclenin (**5**), (+)-iso-gosphorol (**6**), the commercial herbicide Logran® as positive control, and StompAqua® as control for a specific mode of action.
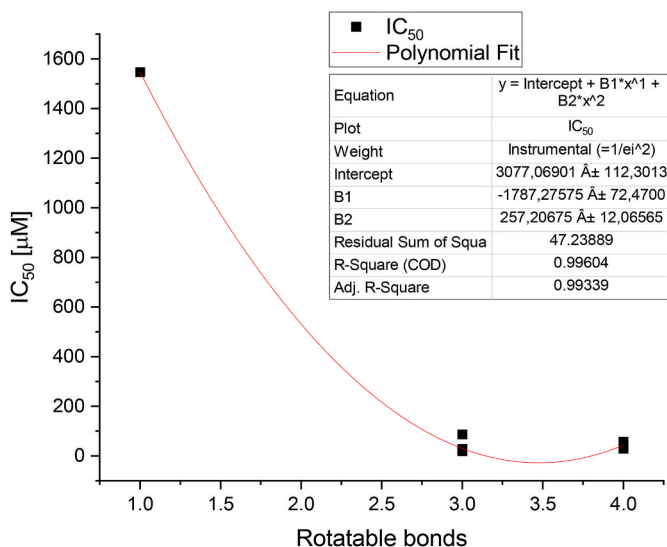

Fig. 3. Representation of IC$_{50}$ values in the coleoptile bioassay vs. rotatable bonds of tested furanocoumarins **1**–**6** according to Hansch's nonlinear model. IC$_{50}$ [µM] = 3077.07–1787.27·(Nº rotatable bonds)+257.21·(Nº rotatable bonds).

2021), which is not so different in terms of total size in comparison with *P.lanceolata*. However, dormancy exert a really important influence in *L. rigidum* germination, and small differences (weeks) in the seed age at the same bank affects to in the allelochemical action (Chauhan et al., 2006). Attending to this, *L. rigidum* germination is extremely sensitive to compounds directly interacting with α-amylase, which is linked to dormancy status (Goggin and Powles, 2012). Furanocoumarins seems

not be involve in this kind of mechanism.

Analyzing the seed germination data for *P. lanceolate* in detail, significant inhibition of seed germination was observed when (+)-oxypeucedanin was applied, with an IC$_{50}$ of 106.60 ± 10.25 µM. However, (+)-heraclenin exhibited a better IC$_{50}$ value of 31.76 ± 0.39 µM. In comparison to the hydroxyl derivative (**4**) and the ether derivative (**1**), the epoxide compounds demonstrated greater influence on germination. (+)-Oxypeucedanin values surpassed the positive control and were significantly (p < 0.01) active at 30 µM.

Root and shoot formation experiments exhibited a more consisted inhibition profile towards the positive control StompAqua® and a similar activity profile for (+)-oxypeucedanin (**3**), yielding values comparable to the positive control StompAqua® at 1000 and 300 µM in terms of root inhibition. The behavior of (+)-heraclenin was slightly different, with stronger inhibition at the two highest tested concentrations (>90%), but a rapid loss of activity at lower concentrations. As predicted by *in silico* tests for TIR1 ubiquitin ligase inhibition, the epoxide showed stronger inhibition than the simple furanocoumarin (**1**) and hydroxyl derivative (**4**). Shoot development displayed the same activity profile as roots.

P. oleracea was also affected by the actions of furanocoumarins. The distinction between epoxide-furanocoumarins and non-epoxide compounds was not as pronounced as in ribwort plantain, but the activity profile remained consistent with the other dicot. Bergapten and (+)-heraclenol did not demonstrate activity against germination, root, or shoot development. In this case, (+)-heraclenin was less active compared to its impact on ribwort plantain. Furthermore, germination was not affected by furanocoumarins, but the inhibition profile for roots and shoots was similar in the case of (+)-oxypeucedanin.

Regarding the structure-activity relationship, *in vitro* and *in vivo* tests indicates the importance of epoxide substructure in weed control. Furthermore, the phytotoxicity bioassay suggest that no epoxide-
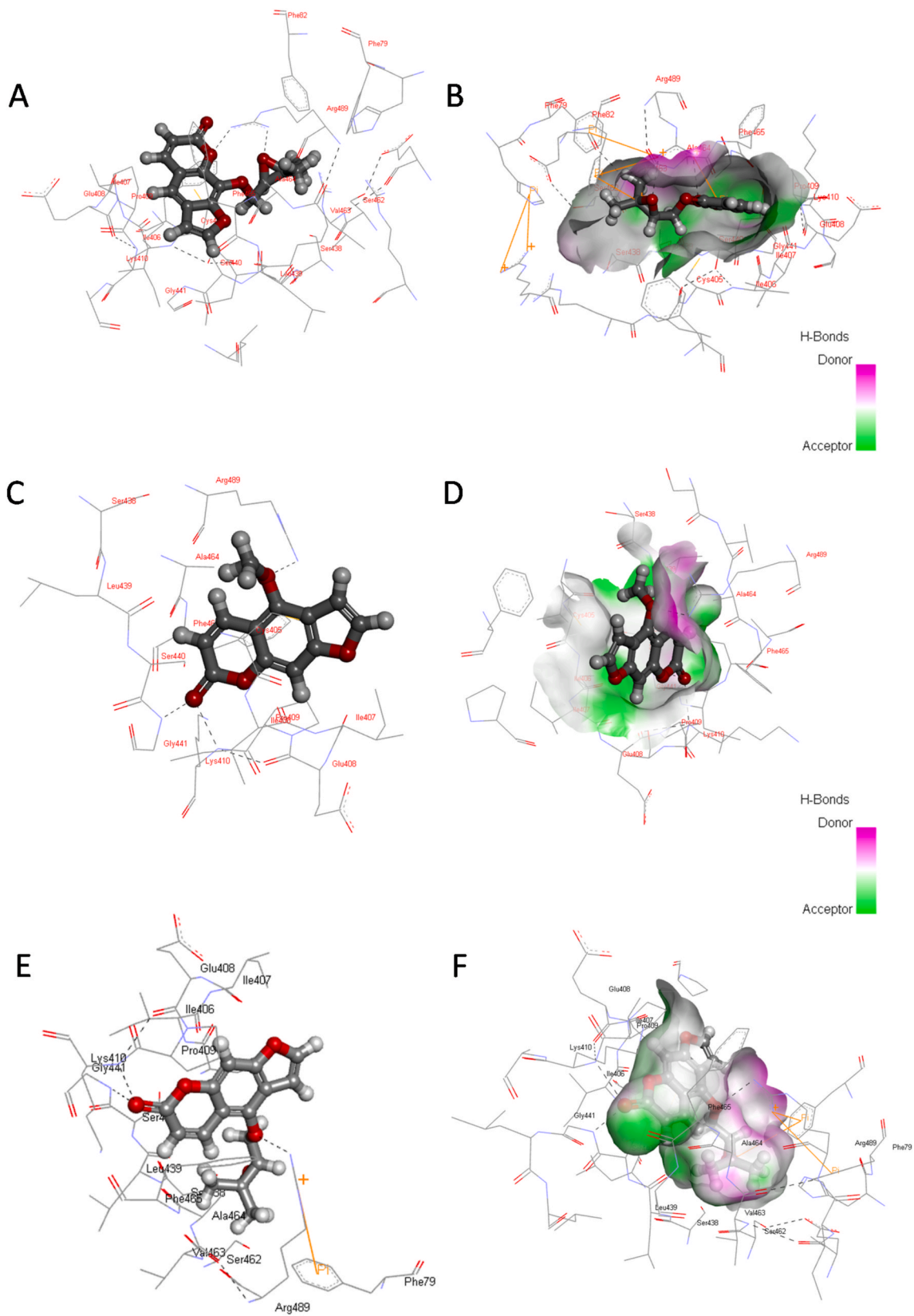
Fig. 4. Suggested interactions of the ligand binding site of TIR1 and (A) (+)-heraclenin (**5**), (C) bergapten (**1**) and (E) (+)-oxypeucedanin (**3**). In addition, surface of electrostatic interactions for (B) (+)-heraclenin (**5**), (D) bergapten (**1**) and (F) (+)-oxypeucedanin (**3**).
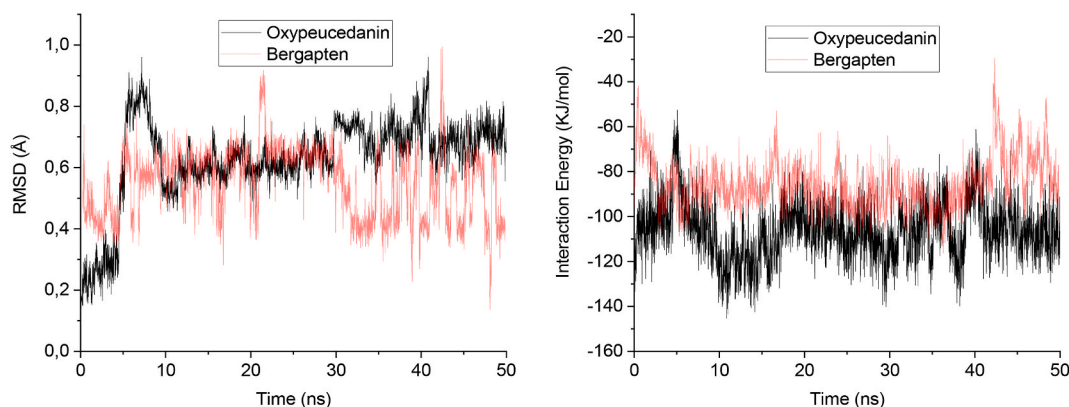
Fig. 5. (Left) Analysis of the Furanocoumarin-TIR1 complex stability along time by RMSD control. (Right) Analysis of the interaction energy per ns of furanocoumarin and TIR1.
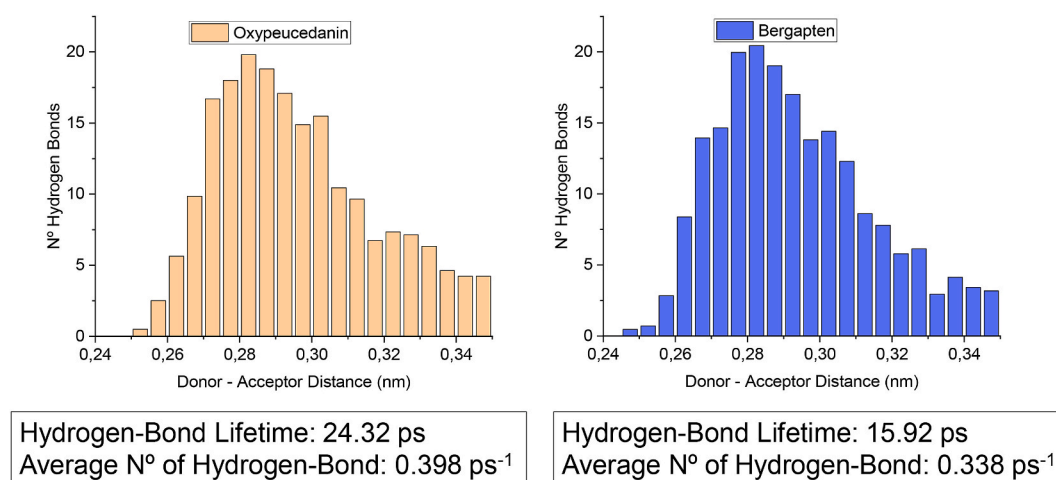

Hydrogen-Bond Lifetime: 24.32 ps
Average Nº of Hydrogen-Bond: 0.398 ps^{-1}

Hydrogen-Bond Lifetime: 15.92 ps
Average Nº of Hydrogen-Bond: 0.338 ps^{-1}

Fig. 6. Analysis of the number of hydrogen bonds of the (+)-oxypeucedanin-TIR1 complex (left) and bergapten-TIR1 complex (right) comparing the number of bonds according to the donor-acceptor distance. In addition, data about bond lifetime and number of hydrogen bonds per picosecond are shown.

opening process would occurs after the incorporation of these molecules into weed plant tissues, due to the observed activity differences of both epoxides (**3** and **5**), which show more inhibition for every parameter (germination, root, and shoots) compared to the corresponding hydroxyl derivative. (+)-Heraclenol and (+)-heraclenin shows similar dipolar moment, and Log*P* values, which would indicate similar bioavailability of the molecules, expecting no such differences in the bioactivity. So, only epoxide arrangement explains the inhibition of the weed parameters.

According to the bioactivity results, and the presence of TIR1 also in the main crops to be protected from the infections with the investigated weeds, a pre-emergency application of *Ducrosia anethifolia* furanocoumarins is suggested. Therefore, isolated furanocoumarins should be applied to the soil prior to crop planting. Alternatively, *Ducrosia anethifolia* might be sowed after harvest of the crop, in a crop rotation method, and after development of the plants mowed/ploughed in order to avoid the development of weeds before next season sowing of the crop. This would avoid negative effects due to TIR1 inhibition in the crop of interest, better than intercropping techniques or post-emergence use.

3. Conclusions

An allelopathic study investigating the biological interactions between furanocoumarins isolated from *Ducrosia anethifolia* and weeds, that affect Mediterranean crops is presented. Six different

furanocoumarins were isolated from the aerial parts of *D. anethifolia*: bergapten, imperatorin, (+)-oxypeucedanin, (+)-heraclenol, (+)-heraclenin, and (+)-isogospherol. Firstly, they were tested in an etiolated wheat coleoptile bioassay to assess general phytotoxicity, and most of the furanocoumarins exhibited strong inhibition of cell elongation. Activity at 1000 μM for (+)-oxypeucedanin, (+)-heraclenol, and (+)-isogospherol was even better than the used positive control. However, the lowest IC$_{50}$ value was observed for (+)-heraclenin, bearing an epoxide side chain at position 8. Hansch's nonlinear model highlighted the significance of rotatable bonds in achieving stronger inhibition against plant cell elongation.

Furanocoumarins seems to act as auxin-like TIR1 ubiquitin ligase inhibitors in plants. *In silico* docking and molecular dynamics simulations were performed to demonstrate the importance of the epoxide substituent in these furanocoumarins. The generated models indicated that a bidental interaction of this group with ester and amino acid residues at the site of action is more effective than other functional groups. Furthermore, when comparing the more biologically active compound with the less active one in the *in silico* model, it was observed that the lifetime of hydrogen bonding is also longer for the more active compound, explaining the better intermolecular interaction with TIR1.

In vitro weed phytotoxicity bioassays were conducted against ribwort plantain (*Plantago lanceolata*), annual ryegrass (*Lolium rigidum*), and common purslane (*Portulaca oleracea*). It was observed that the allelochemicals exhibited species specificity in the germination assay. Specifically, ribwort plantain was highly affected in terms of germination,
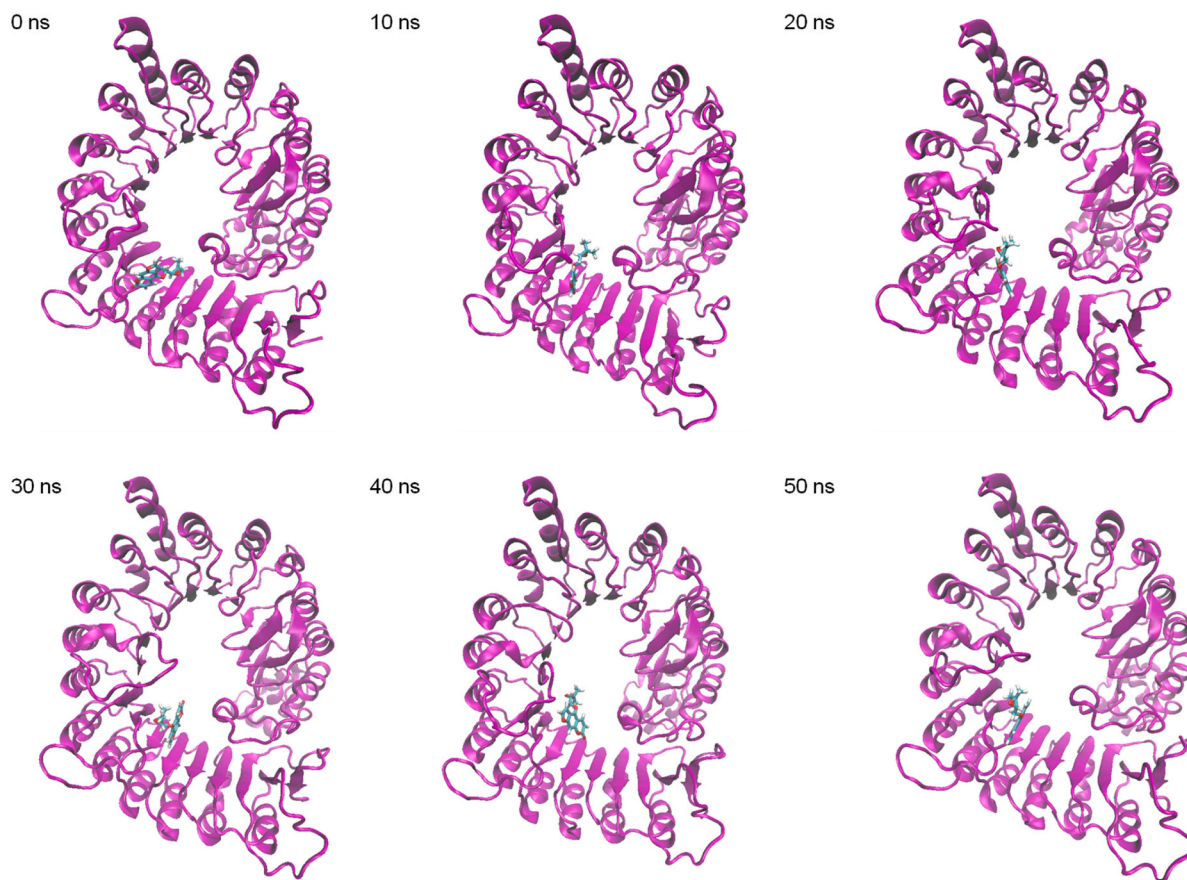
Oxypeucedanin-TIR1

Fig. 7. Snapshot of structural changes at different times of the molecular dynamics for (+)-oxypeucedanin with TIR1 ubiquitin ligase.

root development, and shoot development. Moreover, the bioactivity profile aligned with the *in silico* models related to auxin inhibition, demonstrating that the epoxide derivatives are more active than others and undergo no modification after incorporation into plant tissues.

Main contribution of this research is the first evaluation of furanocoumarins isolated from *D. anethifolia* as potential bioherbicides against ribwort plantain, annual ryegrass, and common purslane. To avoid undesired interactions the application of this plant compounds should be done as pre-emergence intervention, in order to avoid the development of weeds before next season sowing of relevant crops for human consumption.

4. Experimental

4.1. Plant material and isolation of the compounds

The aerial parts of *Ducrosia anethifolia* were collected in the south of Iran (Fars, Neyriz, Iran) (GPS coordinates: 29.149672, 54.275716). Identification of the plant was done by Dr. Mohammad Jamal Saharkhiz at Department of Horticultural Science, Faculty of Agriculture, Shiraz University, Iran, and a voucher specimen was deposited in the Herbarium of Institute of Pharmacognosy, University of Szeged (voucher no.: 880). Aerial parts were dried in shade at room temperature and powdered (3 kg), then extracted with 41 L of methanol. After filtration, the solvent was evaporated to obtain the crude extract. This extract (464.1 g) was dissolved with methanol:water 1:1 (1.5 L) and then subjected to liquid-liquid partitioning using solvents *n*-hexane (4 L), CHCl$_3$ (4 L), EtOAc (4 L), and *n*-BuOH (4 L). After evaporation the solvents *in vacuo*, respectively, *n*-hexane, CHCl$_3$, EtOAc, and *n*-BuOH extracts were

obtained. Isolation of bergapten (**1**), imperatorin (**2**), (+)-oxypeucedanin (**3**), (+)-heraclenol (**4**), (+)-heraclenin (**5**), and (+)-isogospherol (**6**), (Fig. 1), was performed by following the experimental procedure of Mottaghipisheh et al. (2018). NMR data (Figures S7-S12), and optical rotations for absolute configuration, were compared with reported data by Mottaghipisheh et al. (2018).

4.2. Etiolated wheat coleoptile bioassay

The bioassay was carried out following the procedure reported in the literature, with some minor modifications (Macías et al., 2000). Wheat seeds (*Triticum aestivum* L. cv. Burgos) were sown in 15 cm diameter Petri dishes moistened with water and grown in the dark at 25.0 ± 1.0 °C for 4 days. The roots and caryopses were removed from the shoots. The latter were placed in a Van der Weij guillotine and the apical 2 mm were cut off and discarded. The next 4 mm of the coleoptiles were removed and used for bioassays. Every step was performed under a green safelight. All the furanocoumarins were predissolved in dimethyl sulfoxide (0.1%) and diluted in phosphate-citrate buffer containing 2% sucrose at pH 5.6 to the final bioassay concentrations (10^{-3}, 3×10^{-4}, 10^{-4}, 3×10^{-5}, and 10^{-5} M). These conditions were employed also in the control to assure reproducibility and significance.

The commercial herbicide Logran® was employed as positive control. Main active components of this herbicide are of 2-*N*-*tert*-butyl-4-*N*-ethyl-6-methylsulfanyl-1,3,5-triazine-2,4-diamine (terbutryn, 59.4%) and 1-[2-(2-chloroethoxy)phenyl]sulfonyl-3-(4-methoxy-6-methyl-1,3,5-triazin-2-yl)urea (triasulfuron, 0.6%). This reference was used at the same concentrations and under the same conditions than tested compounds. Control samples (buffered aqueous solutions with dimethyl
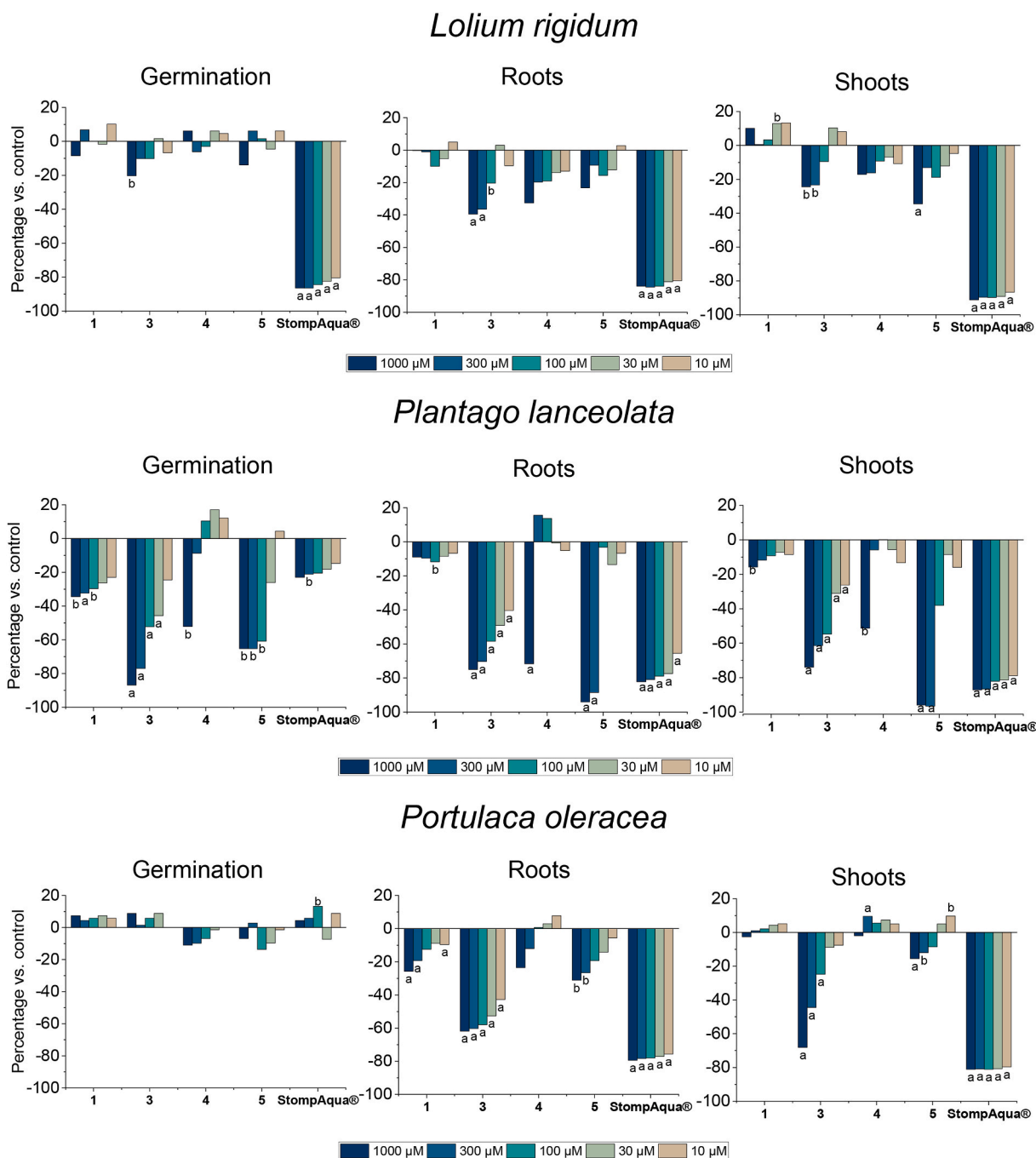
Lolium rigidum

Plantago lanceolata

Portulaca oleracea

Fig. 8. Results of the phytotoxicity bioassay of bergapten (**1**), (+)-oxypeucedanin (**3**), (+)-heraclenol (**4**) and (+)-heraclenin (**5**), against *L. rigidum*, *P. lanceolata*, and *P. oleracea*. Positive values indicate stimulation of growth and negative values indicate inhibition in comparison with the control. Significance levels $p < 0.01$ (a) or $0.01 < p < 0.05$ (b).

sulfoxide and any test compound) were used as negative control to check the activity. Each assay was carried out two times, at different days, and every bioassay has three technical replicates per compound and concentration tested, with five coleoptiles per replicate, prepared from different wheat plants. Every test tube has five coleoptiles and 2 mL of solution, and the tubes were rotated at 0.25 rpm in a roller tube apparatus (Stuart Scientific (Bibby) type SC2 by Thermo-Fischer®, Finland) for 24 h at 25.0 °C in the dark. This is important to avoid photosynthesis during the bioassay. The coleoptiles were measured by digitalization of images with Photomed® (ver. 1.0, University of Cadiz, Spain) after bioassay is finished and data were statistically analyzed. A Welch's *t*-test was developed to determine the significance of the results, with a

significance (*p*-value) fixed at 95% of confidence. This test is a good approach to compare two populations (sample vs. control) that have unequal variances and possibly unequal sample sizes. Data are presented as percentage differences from control. Thus, zero represents the control, positive values represent stimulation of the cell elongation, and negative values represent inhibition of it (Rial et al., 2014).

4.3. *In vitro phytotoxic bioassay*

Three weed species, namely, the monocotyledon annual ryegrass (*Lolium rigidum*), the dicotyledons ribwort plantain (*Plantago lanceolata*) and common purslane (*Portulaca oleracea*), were evaluated as target

plants in this bioassay. *L. rigidum*, *P. oleracea*, and *P. lanceolata* seeds were purchased from Cantueso Natural Seeds (Córdoba, Spain). Bioassays were conducted by following the procedure reported previously, with some modifications (Mejías et al., 2022a,b,c). Petri dishes (50 mm diameter) were used with one sheet of Whatman no. 1 filter paper. Germination and growth were conducted in aqueous solutions at controlled pH using 10^{-2} M of 2-[*N*-morpholino]ethanesulfonic acid and 1 M NaOH (pH 6.0). The compounds to be assayed were dissolved in buffer, and test concentrations of 10^{-3}, 3×10^{-4}, 10^{-4}, 3×10^{-5}, and 10^{-5} M were prepared. 0.05% v/v of dimethyl sulfoxide (DMSO) was applied as co-solvent acting as solubility enhancer. Parallel controls were also run as described previously for coleoptile bioassays. Two different bioassays were performed at different days, and four technical replicates containing 20 seeds were used per bioassay. Treatment, control, or internal reference solution (1 mL) was added to each Petri dish. After adding the seeds and aqueous solutions, the Petri dishes were sealed with Parafilm to ensure closed-system models. Seeds were further incubated at 25 °C in a Memmert ICE 700 controlled environment growth chamber. The photoperiod was 24 h of dark for all weeds. Bioassays took 8 days for every weed, according to what is previously reported (Mejías et al., 2022a). After growth, plants were frozen at −10 °C for 24 h to avoid subsequent growth during the measurement process. The parameters evaluated (germination rate, root length, and shoot length) were recorded using a Fitomed® system (ver. 1.0 University of Cadiz, Spain) (Rial et al., 2014), which allowed automatic data acquisition and statistical analysis using the associated software. Data were analyzed statistically using Welch's test, with significance fixed at 0.01 and 0.05. StompAqua® was employed as positive control. Its composition is based on 3,4-dimethyl-2,6-dinitro-*N*-(pentan-3-yl)aniline (pendimethalin, 45.5%). The results are presented as percentage differences with respect to the control. Zero represents control, positive values represent stimulation, and negative values represent inhibition.

4.4. In silico molecular docking studies

Experiment was performed according to previously published method by Mejias et al. (Mejías et al., 2022a,b,c). The 2D structures of the assayed compounds were generated with ChemBioDraw 20.0 and were converted to 3D structures with GaussView 6.0.16 software (Wallingford, CT, USA). DFT B3LYP/6-311G(d,p) energy minimization was employed prior to carrying out the docking. AutoDockTools (v. 1.5.6) and Autodock 4.2 software were employed to perform this *in silico* study. The protein selected for the docking studies was 2P1P (auxin-like TIR1 ubiquitin ligase) and it was obtained from the Protein Data Bank (www.rcsb.org). A grid box (40 × 40 × 40 Å and 0.575 Å grid points space) was generated and centered on the previous reported binding site for scopoletin (SER438, CYS405 and ARG403) (Graña et al., 2017). Kollman charges were applied to the protein to simulate the electrostatic potential of amino acids. Lamarckian GA algorithm with 50 GA runs were employed to develop the local docking, with a value of 1.0 used as the variance of the Cauchy distribution for gene mutations. All calculations correspond to the most populated cluster, with at least twenty members that fulfill an RMSD tolerance below 2.000 Å. Discovery Studio Visualizer 19.0 was used for the evaluate of the docking results.

4.5. Molecular dynamic studies

The studies were carried out starting from the minimum energy protein–ligand conformation obtained from the previous molecular docking studies. GROMACS (2022.2 version) was employed in conjunction with CHARMM36 force-field (july-2021) and TIP3P water model. The ligand topologies and parameters were obtained using the SwissParam server (www.swissparam.ch). (Zoete et al., 2011) A cubic box was generated and the protein–ligand complex (Furanocoumarin-2P1P) were at least 1 nm from the edges of the box, with a distance of at least 2 nm between periodic images of the protein in order to fulfill the

minimum image convention. A 0.1 M NaCl concentration was simulated in the system to mimic physiological conditions. An energy minimization was applied until the maximum force was less than 10 kJ/mol. The system was then equilibrated for 0.1 ns with 2 fs per step at 300 K using canonical equilibration. Equilibration of the pressure was then carried out by the isothermal–isobaric method using the Parrinello–Rahman barostat. The system was equilibrated for 0.1 ns, also with 2 fs per step, at 300 K. The full equilibrated system was submitted to a molecular dynamics simulation for 50 ns with 2 fs per step. Correction of the trajectory was carried out by protein recentering within the cubic box. Snapshots of the trajectory were collected every 10 ns. RMSD was analyzed to evaluate the stability of the protein-ligand complex. The average number of hydrogen bonds and average distance of these bonds were calculated using a 0.35 nm cut-off distance. Interaction energy between the protein and the furanocoumarins was evaluated as Lenard-Jones potential.

Declaration of competing interest

The authors declare that they have no known competing financial interests or personal relationships that could have appeared to influence the work reported in this paper.

Data availability

No data was used for the research described in the article.

Appendix A. Supplementary data

Supplementary data to this article can be found online at https://doi.org/10.1016/j.phytochem.2023.113838.

References

Banerjee, S.K., Mukhopadhyay, S., Gupta, B.D., Singh, K., Raj, S., 1987. Sesebrinic acid, a cinnamic acid derivative from *Seseli sibiricum*. Phytochemistry 26, 1817–1820. https://doi.org/10.1016/S0031-9422(00)82295-5.

Broster, J., Koetz, E., Wu, H., 2013. Herbicide resistance levels in annual ryegrass (*Lolium rigidum* Gaud.) and wild oat (avena spp.) in southwestern New South Wales. Plant Protect. Q. 28, 126–132.

Cardozo, T., Pagano, M., 2004. The SCF ubiquitin ligase: insights into a molecular machine. Nat. Rev. Mol. Cell Biol. 5, 739–751. https://doi.org/10.1038/nrm1471.

Chauhan, B.S., Gill, G., Preston, C., 2006. Influence of environmental factors on seed germination and seedling emergence of rigid ryegrass (*Lolium rigidum*). Weed Sci. 54, 1004–1012. https://doi.org/10.1614/WS-06-087R.1.

Danin, A., Baker, I., Baker, H.G., 1978. Cytogeography and taxonomy of the *Portulaca oleracea* L. Polyploid complex. Isr. J. Bot. 27, 177–211.

Dharmasiri, N., Dharmasiri, S., Estelle, M., 2005. The F-box protein TIR1 is an auxin receptor. Nature 435, 441–445. https://doi.org/10.1038/nature03543.

Durán, A.G., Chinchilla, N., Molinillo, J.M.G., Macías, F.A., 2018. Influence of lipophilicity in O-acyl and O-alkyl derivatives of juglone and lawsone: a structure–activity relationship study in the search for natural herbicide models. Pest Manag. Sci. 74, 682–694. https://doi.org/10.1002/ps.4764.

European Commission, 2021. Commission Staff Working Document Impact Assessment Report. Accompanying the Document Proposal for a Regulation of the European Parliament and of the Council on the Sustainable Use of Plant Protection Products and Amending Regulation (EU) 2021/2115 [WWW Document]. URL. https://eur-lex.europa.eu/legal-content/EN/TXT/?uri=CELEX%3A52022SC0170&qid=16635805 65339. (Accessed 19 September 2022).

Fendrych, M., Akhmanova, M., Merrin, J., Glanc, M., Hagihara, S., Takahashi, K., Uchida, N., Torii, K.U., Friml, J., 2018. Rapid and reversible root growth inhibition

by TIR1 auxin signalling. Nat. Plants 4, 453–459. https://doi.org/10.1038/s41477-018-0190-1.

Goggin, D.E., Powles, S.B., 2012. Selection for low dormancy in annual ryegrass (*Lolium rigidum*) seeds results in high constitutive expression of a glucose-responsive α-amylase isoform. Ann. Bot. 110, 1641–1650. https://doi.org/10.1093/aob/mcs213.

Graña, E., Costas-Gil, A., Longueira, S., Celeiro, M., Teijeira, M., Reigosa, M.J., Sánchez-Moreiras, A.M., 2017. Auxin-like effects of the natural coumarin scopoletin on Arabidopsis cell structure and morphology. J. Plant Physiol. 218, 45–55. https://doi.org/10.1016/j.jplph.2017.07.007.

Hansch, Corwin, Fujita, Toshio, 1964. p-σ-π analysis. A method for the correlation of biological activity and chemical structure. J. Am. Chem. Soc. 86, 1616–1626. https://doi.org/10.1021/ja01062a035.

Kim, I., 2012. Anatomical and morphological features of seeds in portulaca. Applied Microscopy 42, 194–199. https://doi.org/10.9729/AM.2012.42.4.194.

Macías, F.A., Castellano, D., Molinillo, J.M.G., 2000. Search for a standard phytotoxic bioassay for allelochemicals. Selection of standard target species. J. Agric. Food Chem. 48, 2512–2521. https://doi.org/10.1021/jf9903051.

Macías, F.A., Durán, F.R., Oliveros-Bastidas, A., Castellano, D., Simonet, A.M., Molinillo, J.M.G., 2006. Structure-activity relationship (SAR) studies of benzoxazinones, their degradation products, and analogues. Phytotoxicity on problematic weeds Avena fatua L. and Lolium rigidum Gaud. J. Agric. Food Chem. 54, 1040–1048. https://doi.org/10.1021/jf050903h.

Macías, F.A., Mejías, F.J., Molinillo, J.M., 2019. Recent advances in allelopathy for weed control: from knowledge to applications. Pest Manag. Sci. 75, 2413–2436. https://doi.org/10.1002/ps.5355.

Macías, F.A., Molinillo, J.M., Varela, R.M., Galindo, J.C., 2007. Allelopathy - a natural alternative for weed control. Pest Manag. Sci. 63, 327–348. https://doi.org/10.1002/ps.1342.

Maity, A., Singh, V., Martins, M.B., Ferreira, P.J., Smith, G.R., Bagavathiannan, M., 2021. Species identification and morphological trait diversity assessment in ryegrass (*Lolium* spp.) populations from the Texas Blackland Prairies. Weed Sci. 69, 379–392. https://doi.org/10.1017/wsc.2021.18.

McSteen, P., 2010. Auxin and monocot development. Cold Spring Harbor Perspect. Biol. 2 https://doi.org/10.1101/cshperspect.a001479 a001479–a001479.

Meepagala, K.M., Bracken, A.K., Fronczek, F.R., Johnson, R.D., Wedge, D.E., Duke, S.O., 2021. Furanocoumarin with phytotoxic activity from the leaves of *Amyris elemifera* (rutaceae). ACS Omega 6, 401–407. https://doi.org/10.1021/acsomega.0c04778.

Mejías, Francisco J.R., Carrasco, Á., Durán, A.G., Molinillo, J.M.G., Macías, F.A., Chinchilla, N., 2022a. On the formulation of disulfide herbicides based on aminophenoxazinones: polymeric nanoparticle formulation and cyclodextrin complexation to combat crop yield losses. Pest Manag. Sci. 79, 1547–1556. https://doi.org/10.1002/ps.7327.

Mejías, Francisco J.R., Durán, A.G., Chinchilla, N., Varela, R.M., Álvarez, J.A., Molinillo, J.M.G., García-Cozar, F., Macías, F.A., 2022b. In: In Silico Evaluation of Sesquiterpenes and Benzoxazinoids Phytotoxins against Mpro, RNA Replicase and Spike Protein of SARS-CoV-2 by Molecular Dynamics. Inspired by Nature, vol. 14, p. 599. https://doi.org/10.3390/toxins14090599. Toxins.

Mejías, Francisco J.R., Fernández, I.P., Rial, C., Varela, R.M., Molinillo, J.M.G., Calvino, J.J., Trasobares, S., Macías, F.A., 2022c. Encapsulation of *cynara cardunculus* guaiane-type lactones in fully organic nanotubes enhances their phytotoxic properties. J. Agric. Food Chem. 70, 3644–3653. https://doi.org/10.1021/acs.jafc.1c07806.

Monaco, T.J., Weller, S.C., Ashton, F.M., 2002. Cell growth disrupters and inhibitors. In: Weed Science: Principles and Practices. Wiley-Blackwell, New York, pp. 256–283.

Mottaghipisheh, J., Nové, M., Spengler, G., Kúsz, N., Hohmann, J., Csupora, D., 2018. Antiproliferative and cytotoxic activities of furocoumarins of *Ducrosia anethifolia*. Pharmaceut. Biol. 56, 658–664. https://doi.org/10.1080/13880209.2018.1548625.

Nebo, L., Varela, R.M., Molinillo, J.M.G., Sampaio, O.M., Severino, V.G.P., Cazal, C.M., Fernandes, M.F.D.G., Fernandes, J.B., Macías, F.A., 2014. Phytotoxicity of alkaloids, coumarins and flavonoids isolated from 11 species belonging to the Rutaceae and

Meliaceae families. Phytochem. Lett. 8, 226–232. https://doi.org/10.1016/j.phytol.2014.02.010.

Oueslati, M.H., Bouajila, J., Belkacem, M.A., Harrath, A.H., Alwasel, S.H., Ben Jannet, H., 2019. Cytotoxicity of new secondary metabolites, fatty acids and tocols composition of seeds of *Ducrosia anethifolia* (DC.) Boiss. Nat. Prod. Res. 33, 708–714. https://doi.org/10.1080/14786419.2017.1408101.

Rial, C., Novaes, P., Varela, R.M., Molinillo, J.M.G., Macias, F.A., 2014. Phytotoxicity of cardoon (*Cynara cardunculus*) allelochemicals on standard target species and weeds. J. Agric. Food Chem. 62, 6699–6706. https://doi.org/10.1021/jf501976h.

Royal Botanic Garden, 2023a. Plantago lanceolata L. [WWW Document]. URL https://powo.science.kew.org/taxon/urn:lsid:ipni:names:321285-2#source-KBD. (Accessed 2 September 2023).

Royal Botanic Garden, 2023b. Portulaca oleracea L. [WWW Document]. Royal Botanic Garden. URL https://powo.science.kew.org/taxon/urn:lsid:ipni:org:names:323270-2. (Accessed 2 September 2023).

Russell, T.R., Lulis, T.T., Aynardi, B.A., Tang, K.T., Kaminski, J.E., 2021. Buckhorn plantain (Plantago lanceolata) resistant to 2,4-D in Pennsylvania and alternative control options. Weed Technol. 35, 297–303. https://doi.org/10.1017/wet.2020.116.

Setzer, W.N., Vogler, B., Bates, R.B., Schmidt, J.M., Dicus, C.W., Nakkiew, P., Haber, W.A., 2003. HPLC-NMR/HPLC-MS analysis of the bark extract of *Stauranthus perforatus*. Phytochem. Anal. 14, 54–59. https://doi.org/10.1002/pca.687.

Shalaby, N.M.M., Abd-Alla, H.I., Aly, H.F., Albalawy, M.A., Shaker, K.H., Bouajila, J., 2014. Preliminary *in vitro* and *in vivo* evaluation of antidiabetic activity of *Ducrosia anethifolia* boiss. And its linear furanocoumarins. BioMed Res. Int. 1–13. https://doi.org/10.1155/2014/480545, 2014.

Sondhia, S., Duke, S.O., Green, S., Gemejiyeva, N.G., Mamonov, L.K., Cantrell, C.L., 2012. Phytotoxic furanocoumarins from the shoots of *Semenovia transiliensis*. Nat. Prod. Commun. 7 https://doi.org/10.1177/1934578X1200701019, 1934578X1200701.

Stevenson, P.C., Simmonds, M.S.J., Yule, M.A., Veitch, N.C., Kite, G.C., Irwin, D., Legg, M., 2003. Insect antifeedant furanocoumarins from *Tetradium daniellii*. Phytochemistry 63, 41–46. https://doi.org/10.1016/S0031-9422(02)00748-3.

Sultana, N., Sultana, R., 2009. A new lanostane triterpene from *Skimmia laureola*. Z. Naturforsch. B Chem. Sci. 64, 459–463. https://doi.org/10.1515/znb-2009-0418.

Tabaglio, V., Gavazzi, C., Schulz, M., Marocco, A., 2008. Alternative weed control using the allelopathic effect of natural benzoxazinoids from rye mulch. Agron. Sustain. Dev. 28, 397–401. https://doi.org/10.1051/agro:2008004.

Verma, A.K., Kumar Avinash Bharti, N.G., 2017. Macro and micro-morphological characteristics of Plantago seeds and its implication for species identification. Curr. Bot. 8 https://doi.org/10.19071/cb.2017.v8.3243.

Walsh, T.A., Neal, R., Merlo, A.O., Honma, M., Hicks, G.R., Wolff, K., Matsumura, W., Davies, J.P., 2006. Mutations in an auxin receptor homolog AFB5 and in SGT1b confer resistance to synthetic picolinate auxins and not to 2,4-dichlorophenoxyacetic acid or indole-3-acetic acid in Arabidopsis. Plant Physiol. 142, 542–552. https://doi.org/10.1104/pp.106.085969.

Wei, Y., Ito, Y., 2006. Preparative isolation of imperatorin, oxypeucedanin and isoimperatorin from traditional Chinese herb "Bai zhi" *Angelica dahurica* (Fisch. ex Hoffm) Benth. et Hook using multidimensional high-speed counter-current chromatography. J. Chromatogr. A 1115, 112–117. https://doi.org/10.1016/j.chroma.2006.02.081.

Yadav, R.P., Syed Ibrahim, K., Gurusubramanian, G., Senthil Kumar, N., 2015. *In silico* docking studies of non-azadirachtin limonoids against ecdysone receptor of *Helicoverpa armigera* (Hubner) (Lepidoptera: noctuidae). Med. Chem. Res. 24, 2621–2631. https://doi.org/10.1007/s00044-015-1320-1.

Yang, H., Zhou, S., Wu, L., Wang, L., 2022. Interference of dihydrocoumarin with hormone transduction and phenylpropanoid biosynthesis inhibits barnyardgrass (*Echinochloa crus-galli*) root growth. Plants 11, 2505. https://doi.org/10.3390/plants11192505.

Zoete, V., Cuendet, M.A., Grosdidier, A., Michielin, O., 2011. SwissParam: a fast force field generation tool for small organic molecules. J. Comput. Chem. 32, 2359–2368. https://doi.org/10.1002/jcc.21816.